FULL PAPER

Dalton
www.rsc.org/dalton

Temperature dependence of the crystal structure and luminescence properties of [Pt{4′-(*o*-ClC_6H_4)trpy}Cl]SbF_6 (trpy = 2,2′:6′,2″-terpyridine)†

John S. Field,*[a] Jan-Andre Gertenbach,[a] Raymond J. Haines,[a] Lesibana P. Ledwaba,[a] Ndoda T. Mashapa,[a] David R. McMillin,[b] Orde Q. Munro[a] and Grant C. Summerton[a]

[a] *School of Chemical and Physical Sciences, University of Natal, Private Bag X01, Pietermaritzburg 3201, South Africa. E-mail: fieldj@nu.ac.za*

[b] *Department of Chemistry, Purdue University, West Lafayette, Indiana 47907-1393, USA. E-mail: mcmillin@purdue.edu*

Received 4th October 2002, Accepted 9th January 2003
First published as an Advance Article on the web 11th February 2003

The synthesis and characterisation of 4′-(2‴-chlorophenyl)-2,2′:6′,2″-terpyridine [4′-(*o*-ClC_6H_4)trpy] and [Pt{4′-(*o*-ClC_6H_4)trpy}Cl]SbF_6 are described. An X-ray crystal structure determination of the salt reveals columns of cations and anions with the cations stacked parallel and head-to-tail. At 295 K the Pt ⋯ Pt distances alternate between 3.374(1) and 3.513(1) Å while the perpendicular separation between the mean planes comprising the platinum and three bonded nitrogen atoms remains constant at 3.35 Å. As evidenced by crystal structure determinations at 260, 240 and 180 K, the shorter Pt ⋯ Pt distances become systematically shorter and the longer Pt ⋯ Pt distances become systematically longer as the temperature of the crystal is lowered. Structural evidence is presented that shows that this trend is a consequence of the more closely separated platinum atoms slipping into line with respect to a perpendicular to the above planes; at the same time the more widely separated platinum atoms fall out-of-line as the temperature is lowered. Emission spectra measured on a polycrystalline sample of the salt at 40 K intervals from 280 to 80 K comprise a single, asymmetric and featureless band [λ_{max}^{em} = 609 nm at 280 K] that systematically increases in intensity as the temperature is lowered. There is a slight blue shift in the wavelength of the emission maximum as the temperature is lowered to 240 K but, below this temperature, the emission maximum gradually and systematically shifts to the red [λ_{max}^{em} = 642 nm at 80 K]. This behaviour is rationalised in terms of ^{3}MMLCT emission, the energy of which being determined by subtle changes in the extent of d_{z^2}–d_{z^2} orbital overlap between adjacent platinum atoms separated by the shorter distance on one hand, and between platinum atoms separated by the longer distance on the other.

Introduction

Polypyridyl ligand complexes of platinum(II) have received considerable attention insofar as their luminescence properties are concerned.[1–10] Of interest here are those materials that have planar chromophores stacked in the solid state with significant electronic interactions between them. Well-studied examples are the red α-diimine complexes [$PtCl_2$(bpy)][2,8] (bpy = 2,2′-bipyridine), [$Pt(CN)_2$(bpy)][11,12] and [$Pt(CN)_2$(*i*-biq)][13] (*i*-biq = 3,3′-biisoquinoline). These three compounds have in common linear chain structures in the solid state *i.e.*, platinum atoms that are equally spaced along an infinite stack, and emission that is assigned as ^{3}MMLCT [dσ*(Pt)–π*(bpy/*i*-biq)]. A distinguishing feature of the emission is that it is red-shifted when the temperature of the sample is lowered. This is explained by the decrease in the Pt–Pt distance that occurs on cooling, as well as by a linear relationship between the emission energy and the inverse of the cube of the Pt–Pt distance of the type originally determined by Gliemann *et al.*, for the tetracyanoplatinates.[8,13,14] The red terpyridyl ligand complex [Pt{4′-(*o*-$CH_3C_6H_4$)trpy}Cl]SbF_6 also possesses a linear chain structure and similarly exhibits ^{3}MMLCT emission that is red-shifted as the temperature of the sample is lowered.[15]

On the other hand all other known terpyridyl ligand complexes of platinum(II) that have a chloro-group as the fourth ligand and for which crystal structures have been reported do not have linear chain structures. For example, the red [Pt(4′-(Ph)trpy)Cl]BF_4·CH_3CN salt has the cations stacked as tetramers in the solid state.[10] Nevertheless, this salt exhibits ^{3}MMLCT emission with a red-shift in the emission maximum on cooling.[10] The triflate[6] and orange perchlorate[7] salts of the [Pt(trpy)Cl]$^+$ cation exhibit dimeric structures, *i.e.*, where the cations are stacked as metal–metal bonded pairs in an infinite π-stack. Interestingly, whereas a red shift in the emission maximum of 25 nm is observed on cooling the triflate salt from room temperature to 77 K,[6,9] there is very slight blue shift of 5 nm in the emission energy (λ_{max}) when the perchlorate salt is cooled from 300 to 77 K.[7] A fourth example is the tetrafluoroborate salt of the [Pt{4′-(*o*-$CH_3C_6H_4$)trpy}Cl]$^+$ cation, a yellow compound that has alternating Pt ⋯ Pt distances that are too long to support d_{z^2}–d_{z^2} interactions between the platinum atoms and that, for this reason, exhibits excimeric π–π* rather than ^{3}MMLCT emission.[15]

We report here the temperature dependence of the crystal structure and solid state emission spectrum of [Pt{4′-(*o*-ClC_6H_4)trpy}Cl]SbF_6. A very small but discernible blue shift in λ_{max} is initially observed on cooling the sample from room temperature to 240 K but, at temperatures below 240 K, there is a systematic shift to the red in the emission maximum as the temperature is lowered. It is in an attempt to gain a better understanding of the temperature dependence of the solid emission by this salt that we have determined the crystal structure of [Pt{4′-(*o*-ClC_6H_4)trpy}Cl]SbF_6 over a range of temperatures. Specifically we wished to establish how the intermolecular Pt–Pt distances change on cooling the sample since, as noted above, these are linked to the emission energy. We note that changes in intermolecular Pt–Pt distances and hence the emission can also be induced by changing the solvent, both in solution[16] and in the solid state.[17]

† Electronic supplementary information (ESI) available: Fig. S1: Unit cell contents of [Pt{4′-(*o*-ClC_6H_4)trpy}Cl]SbF_6 viewed down the [*a*]-axis and Fig. S2: View of the cation stack in [Pt{4′-(*o*-ClC_6H_4)trpy}-Cl]SbF_6. See http://www.rsc.org/suppdata/dt/b2/b209754k/

DOI: 10.1039/b209754k

Results and discussion

The method of Kröhnke,[18] suitably modified,[15] was employed for the synthesis of 4′-(2‴-chlorophenyl)-2,2′:6′,2″-terpyridine [4′-(*o*-ClC_6H_4)trpy]. Full details of the synthetic procedures as well as of the characterisation data for the chalcone intermediate and for the ligand itself are given in the Experimental section. The preparation of the complex follows procedures previously used in our laboratories.[9,10,15] Thus treatment of a refluxing acetonitrile solution of $[Pt(PhCN)_2Cl_2]$ with one equivalent of $AgSbF_6$ afforded a yellow solution and a white precipitate of silver chloride. After removal of the silver chloride one equivalent of the ligand was added to afford the desired product as an analytically pure and air-stable orange crystalline solid. Full characterisation data are given in the Experimental section.

Crystal structure of [Pt{4′-(*o*-ClC_6H_4)trpy}Cl]SbF_6 at 295 K

A perspective view of the cation is given in Fig. 1 with a selection of interatomic distances and angles being listed in the caption. The coordination geometry of the platinum atom is irregular square-planar, deviations from the idealised geometry being evident in the N(1)–Pt–N(2) and N(2)–Pt–N(3) angles of 81.1(3) and 80.8(3)°, respectively. This is due to the geometric constraints imposed by the tridentate ligand and is typical of terpyridyl ligand complexes of platinum(II).[6,7,9,10,19] Also characteristic of a coordinated terpyridyl ligand is that the platinum to bridgehead nitrogen [N(2)] distance of 1.936(6) Å is significantly shorter than the two platinum to outer nitrogen distances of 2.013(6) [N(1)] and 2.018(6) Å [N(3)], respectively.[6,7,9,10,19] The *o*-ClC_6H_4 moiety is twisted about the C(8)–C(16) bond, as reflected by a dihedral angle of 54.5(2)° between the mean plane through the non-hydrogen atoms of the 4′-substituent on one hand and the mean plane through the non-hydrogen atoms of the terpyridyl moiety on the other. This twist is a consequence of steric interactions between the chlorine atom and a hydrogen atom of the central pyridine ring that is also *ortho* with respect to the interannular bond. All other structural features of the isolated cation are entirely as expected.

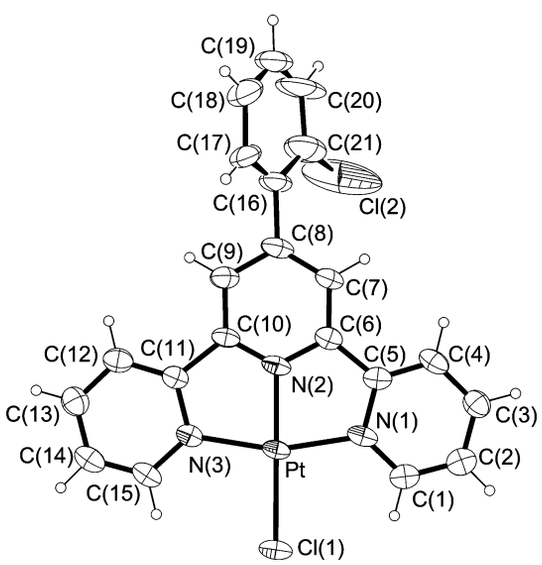

Fig. 1 ORTEP view (40% thermal ellipsoids) of the cation in [Pt{4′-(*o*-ClC_6H_4)trpy}Cl]SbF_6. Selected interatomic distances (Å) and angles (°): Pt–Cl(1) 2.230(2), Pt–N(1) 2.013(6), Pt–N(2) 1.936(4), Pt–N(3) 2.018(6); Cl(1)–Pt–N(1) 99.2(2), Cl(1)–Pt–N(2) 179.7(2), Cl(1)–Pt–N(3) 98.9(2), N(1)–Pt–N(2) 81.1(2), N(1)–Pt–N(3) 161.9(2), N(2)–Pt–N(3) 80.8(3).

The crystal structure of [Pt{4′-(*o*-ClC_6H_4)trpy}Cl]SbF_6 consists of separate columns of cations and anions that are aligned along the [*a*]-axis of the unit cell (Fig. S1). Of particular interest are the details of how the cations are stacked within a column. We first note that successive cations are related by centres of inversion that repeat at half-intervals along the [*a*]-axis. This ensures that the cation planes, specifically the mean planes through the platinum and three bonded nitrogen atoms, are parallel and that the cations stack head-to-tail (Fig. S2). Secondly, the platinum atoms zigzag about the [*a*]-axis as indicated by a Pt ··· Pt ··· Pt angle of 167.1(1)° and, thirdly, the [*a*]-axis is at an angle of *ca.* 16° to the normal to the cation planes. With regard to the Pt ··· Pt distances, these alternate in length along the stack, adopting values of 3.374(1) and 3.513(1) Å in the 295 K structure. The perpendicular separation between successive mean planes defined by the Pt, N(1), N(2) and N(3) atoms (the interplanar spacing) remains constant along the stack with a value of 3.35 Å at 295 K. Thus, the difference in the Pt ··· Pt distances is a result of the platinum atoms of successive pairs of cations being slipped to different extents with respect to a line drawn perpendicular to the platinum coordination plane. Fig. 2 illustrates the two different cation–cation interactions along the stack taking a view perpendicular to the mean plane through the platinum atom and the nitrogen atoms bonded to it. Note that the direction of the *o*-ClC_6H_4 moiety twist about the C(8)–C(16) bond is such that the chlorines point *between* the cations making up the more widely separated pair (Fig. 2B) whereas they point *away* from the adjacent cation for the more closely separated pair (Fig. 2A).

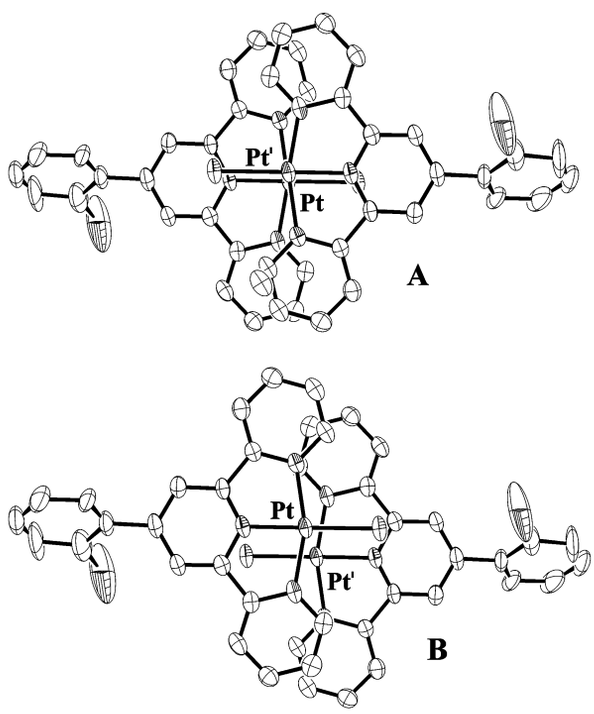

Fig. 2 ORTEP diagrams (20% thermal ellipsoids) showing the two types of cation–cation interactions along the cation stacks in [Pt{4′-(*o*-ClC_6H_4)trpy}Cl]SbF_6 viewed perpendicular to the mean planes through the platinum atom and the three nitrogen atoms bonded to it: A, Pt ··· Pt = 3.374(1) Å (at 295 K); B, Pt ··· Pt = 3.513(1) Å (at 295 K).

Though the Pt ··· Pt distances alternate along the stack and the shorter of the distances of 3.374(1) Å certainly allows for a significant d_{z^2}–d_{z^2} interaction, the cation stacking is not strictly classified as that of a dimeric structure as reported for the triflate[6] and orange perchlorate[7] salts of the $[Pt(trpy)Cl]^+$ cation. The reason is that the longer distance of 3.513(1) Å is close to the value of *ca.* 3.5 Å, usually taken to be the upper limit for a significant d_{z^2}–d_{z^2} interaction between two platinum atoms,[20] and so cannot be ignored. The cation stacking is thus probably best described as intermediate between that of a linear chain

Table 1 Crystal and refinement data for [Pt{4(*o*-ClC_6H_4)trpy}Cl]SbF_6[a]

	295 K	260 K	240 K	180 K
a/Å	6.844(1)	6.821(1)	6.818(1)	6.787(2)
b/Å	18.965(2)	18.889(4)	18.863(5)	18.804(11)
c/Å	18.333(3)	18.302(3)	18.276(4)	18.221(8)
β/°	90.05(1)	90.05(1)	90.0(2)	91.38(4)
V/Å^3	2379.6(6)	2358.0(7)	2350.5(9)	2325(2)
D_c/g cm^{-3}	2.261	2.282	2.289	2.315
Total no. of reflns. measured	5764	5879	8909	5568
Independent reflns.	4174	4132	4116	4066
R_{int}	0.016	0.041	0.029	0.021
Reflections observed [$I > 2\sigma(I)$]	3290	3233	3474	3583
R_1[b] [$I > 2\sigma(I)$]	0.037	0.042	0.041	0.057
R_1[b], wR_2[c] (all data)	0.049, 0.117	0.056, 0.129	0.051, 0.139	0.063, 0.189
No. of refined parameters, restraints	308, 0	308, 0	308, 0	308, 0
(Shift/esd)$_{max}$	0.002	0.001	0.013	0.002
Max. $\Delta\rho$/e Å^{-3}	2.19 [Pt]	2.43 [Pt]	2.60 [Cl(2)]	4.62 [Cl(2)]
Min. $\Delta\rho$/e Å^{-3}	−1.52 [N(2)]	−1.80 [N(2)]	−2.18 [Cl(2)]	−4.67 [Cl(2)]

[a] Crystal data common to all temperatures: formula (M_w), $C_{21}H_{14}Cl_2F_6N_3PtSb$ (810.09); crystal system, monoclinic; space group, $P2_1/n$ (no. 14); $Z = 4$; $F(000) = 1512$; $\mu = 7.29$ mm^{-1}; refinement on F^2. [b] $R_1 = \Sigma||F_o| - |F_c||/\Sigma|F_o|$. [c] $wR_2 = [\Sigma[w(F_o^2 - F_c^2)^2]/\Sigma[w(F_o^2)^2]]^{1/2}$ where $w = 1/[\sigma^2(F_o^2) + (0.1P)^2]$ and $P = (F_o^2 + 2F_c^2)/3$.

structure and that of a dimeric structure. Indeed, it is the first example of a structure that represents the interface between the two extremes of a linear chain structure on one hand and a truly dimeric structure on the other. As discussed below, this has consequences for the temperature dependent emission behaviour of the compound.

Photophysical and low-temperature crystal structure studies

The absorption spectrum of [Pt{4′-(*o*-ClC_6H_4)trpy}Cl]SbF_6 measured in acetonitrile is very similar to those recorded in the same solvent for salts of the closely-related $[Pt(trpy)Cl]^+$ and $[Pt\{4'\text{-}(RC_6H_4)trpy)\}Cl]^+$ (R = H, CH_3 and CF_3) chromophores.[6,7,10] Accordingly, the same assignments are made. The strong band at 284 nm and the vibrationally structured band with maxima in the range 300–360 nm are attributed to $^1(\pi\text{–}\pi)$ transitions of the substituted terpyridyl ligand, while the two less intense and poorly resolved peaks at wavelengths greater than 380 nm are assigned to Pt(5d) ⟶ trpy(π*) (^{1}MLCT) transitions. Data are given in the Experimental section. The compound does not give rise to detectable emission when dissolved in degassed acetonitrile and irradiated with light of 330 nm wavelength at room temperature. Quenching of the fluid emission is probably due to coordination of the donor solvent to the platinum atom in an axial position.[21] Unfortunately, because of solubility problems, it was not possible to measure emission spectra in a non-coordinating solvent such as dichloromethane.

Emission spectra measured over a range of temperatures on a microcrystalline sample of the [Pt{4′-(*o*-ClC_6H_4)trpy}Cl]SbF_6 salt are shown in Fig. 3. A single asymmetric band that increases in intensity and decreases in width as the temperature is lowered is observed. The lack of vibrational structure, the relative narrowness of the band (fwhm = 1595 and 1219 cm^{-1} at 280 and 80 K, respectively) and the lifetime (259 and 2150 ns at 295 and 77 K respectively) are typical of ^{3}MMLCT emission. This assignment is also consistent with the presence of platinum d_{z^2}–d_{z^2} interactions in the crystal (*vide supra*). Of particular interest is that there is a slight but discernible blue shift of *ca.* 10 nm in the emission maximum when the temperature is lowered from 280 to 240 K. Thereafter the wavelength of the emission maximum gradually and systematically increases from a value of 619 nm at 240 K to 642 nm at 80 K. The initial blue shift is unexpected. In nearly all studies of the temperature dependence of solid ^{3}MMLCT emission by bipyridyl and terpyridyl ligand complexes of platinum(II) a *red* shift in the emission maximum is observed when the temperature is lowered.[1,6,8,11,13] This red shift has been associated with a shortening of the Pt ··· Pt

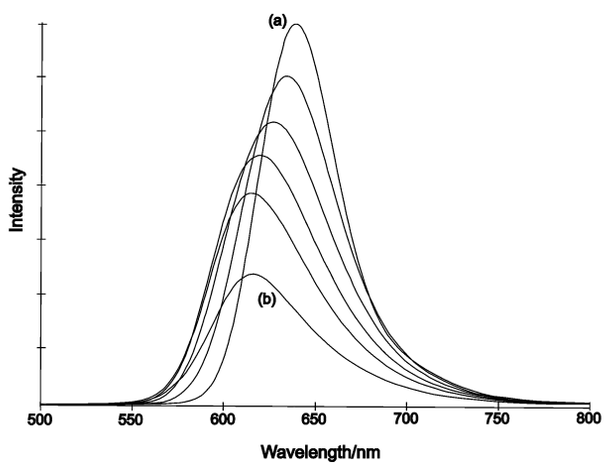

Fig. 3 Solid state emission spectra of [Pt{4′-(*o*-ClC_6H_4)trpy}Cl]SbF_6 recorded at 40 K intervals over the range 80 K (a) to 280 K (b): $\lambda_{ex} = 330$ nm.

distances due to unit cell contraction as the temperature of the crystal is lowered.[8,11] One exception is the orange salt $[Pt(trpy)Cl]ClO_4$ that has been shown to exhibit a very slight blue shift of 5 nm in the emission maximum (λ_{max}) when the salt is cooled from 300 to 77 K.[7]

In order to try and understand the temperature dependence of the solid emission by [Pt{4′-(*o*-ClC_6H_4)trpy}Cl]SbF_6 we have also determined the crystal structure of the compound at 260, 240 and 180 K. Crystal and refinement data for the room temperature and three low temperature structures are given in Table 1. Two observations follow from the data in Table 1. Firstly, there is no phase change on cooling. Secondly, there is a systematic decrease in the unit cell volume with an approximately equal decrease of about 0.7 % in the lengths of each of the unit cell axes over the full temperature range *i.e.*, the contraction of the unit cell is essentially isotropic. Structural results pertinent to the following discussion are listed in Table 2. Insofar as the Pt ··· Pt distances are concerned these exhibit the following trend on cooling: the shorter distance becomes systematically shorter while the longer distance becomes systematically longer. With regard to the interplanar spacing, this shows a very small reduction as the temperature of the crystal is lowered from 295 to 180 K. We conclude: as the temperature is lowered the closer platinum atoms slip into line with respect to a perpendicular to the stacking planes, and so get closer together, while the more distant platinum atoms slip out-of-line, and so get further apart. This is

Table 2 Structural data for [Pt{4′-(*o*-ClC_6H_4)trpy}Cl]SbF_6

	295 K	260 K	240 K	180 K
Pt–Pt/Å	3.374(1)	3.352(1)	3.344(1)	3.311(1)
	3.513(1)	3.523(1)	3.533(1)	3.550(1)
Pt–Pt–Pt/°	167.1(1)	165.7(1)	164.0(1)	163.1(1)
Interplanar spacing[a]/Å	3.35	3.33	3.33	3.31
	3.35	3.34	3.32	3.30
Lateral offset[b]/Å	0.40	0.36	0.27	0.00
	1.05	1.13	1.20	1.32

[a] The interplanar spacing is defined as the averaged perpendicular distance between adjacent mean planes calculated through Pt, N1, N2 and N3. The first value is the distance between planes linked by the shorter Pt–Pt distance, the second is the distance between planes linked by the longer Pt–Pt distance. It is unlikely that any small differences between the two values are significant. [b] The lateral offset was calculated as the length of the third side in a right-angled triangle with a hypotenuse equal to the Pt–Pt distance and the second side equal to the interplanar spacing as defined above.

confirmed by an analysis of how the lateral offset between two adjacent platinum atoms changes on cooling. The data show a systematic decrease in the lateral offset for the closer platinum atoms and a corresponding increase in the lateral offset for the more distant platinum atoms as the temperature is lowered.

How do the above changes in the Pt ⋯ Pt distances relate to the observed shifts in the emission maximum brought about by cooling the sample? Given that there is an initial blue shift in the emission maximum the implication is that there is an initial widening of the band gap when the temperature is lowered from room temperature to *ca.* 240 K. We suggest that this increase in the band gap is the result of a weakening of the already weak (but finite) d_{z^2}–d_{z^2} interactions between the more distant platinum atoms that occurs when the longer Pt ⋯ Pt distance gets longer. Below 240 K this second d_{z^2}–d_{z^2} interaction plays no role in determining the energies of the highest occupied and lowest unoccupied orbitals, and the analysis becomes one of a series of molecular metal–metal bonded dimers. As has been well-established for platinum dimers that exhibit ^{3}MMLCT emission, a shortening of the distance between the two metal atoms is expected to result in a closing of the HOMO–LUMO gap and a red-shift in the emission maximum.[1,8,11] As noted above and illustrated in Fig. 3, this is indeed the observed trend below 240 K.

Concluding remarks

Connick *et al.* have noted that a major contribution to the stability of linear chain structures of polypyridyl ligand complexes of platinum(II) is the platinum d_{z^2}–d_{z^2} interaction that extends perpendicular to the stack.[22] A shortening of the Pt ⋯ Pt distances brought about by cooling the sample is expected to lead to an increase in the d_{z^2}–d_{z^2} interactions and a concomitant further stabilisation of the linear chain structure. (We note in parentheses that this will only be true provided the d_{z^2}-orbitals remain suitably oriented for overlap.) It is therefore of interest to note that when crystals of [Pt{4′-(*o*-ClC_6H_4)-trpy}Cl]SbF_6 are cooled the Pt ⋯ Pt distances change in such a way that a linear chain structure is *not* formed; instead a dimeric structure is adopted at lower temperatures. It follows that the dimeric structure is the preferred one at lower temperatures. This is consistent with Peierls theorem that states that one-dimensional structures with equal separations of the repeating units are not intrinsically stable and that, as the temperature of the material is lowered, distortions are anticipated that will lead to the formation of molecular units along the stack.[23] In this case the distortions take the form of the platinum atoms slipping into different positions with respect to a line perpendicular to the cation stack.

Experimental

Materials

Reagents for the ligand synthesis were obtained and used as follows: The 2-acetylpyridine (Fluka) and 2-chlorobenzaldehyde (Merck) were obtained commercially and used without further purification while the *N*-{1-(2′-pyridyl)-1-oxo-2-ethyl-}pyridinium iodide was synthesised by the method of Kröhnke.[18] All manipulations for the complex salt syntheses were performed under an atmosphere of nitrogen using standard Schlenk tube techniques. The acetonitrile used as the solvent and for the purposes of crystal growth was purified by the method of Carlsen and Anderson.[24] The dichlorobis(benzonitrile)platinum(II) (Strem) and the silver salt $AgSbF_6$ (Fluka) were used without further purification.

Physical measurements and instrumentation

Microanalyses for %C, H and N were performed by Galbraith Laboratories Inc., Knoxville, Tennessee, USA. Melting points were recorded on a Kofler hot stage apparatus and are uncorrected. ^{1}H NMR (200 MHz) spectra were recorded on a Varian Gemini 200 spectrometer at 25 °C with chemical shifts referenced to $SiMe_4$. IR spectra were recorded as KBr discs on a Shimadzu FTIR-4300 spectrometer. Mass spectra were obtained on a Hewlett Packard GCMS using electron impact (EI) ionisation. UV-vis absorption spectra were recorded at 22 °C using a Shimadzu UV-2101PC scanning spectrophotometer. Emission spectra were recorded on a SLM-Amico SPF 500C fluorometer at 22 °C unless otherwise stated. Deoxygenated spectroscopic grade solvents were used for both the absorption and emission measurements. Solid-state emission spectra were recorded on microcrystalline samples. For the variable-temperature emission measurements the cryostat was an Oxford Instruments DN1704 liquid-nitrogen-cooled system complete with an Oxford Instruments temperature controller. The excitation wavelength was 330 nm, with the scattered light removed by a 400 nm long-wave-pass filter. The 337 nm line from a nitrogen laser served as the excitation source for the lifetime measurements, with a 337 nm band pass filter used to remove stray light from the beam. Lifetime data were analysed as described previously.[25]

Syntheses

2-Chloro-1-{3-(2-pyridyl)-3-oxopropenyl}benzene. A solution of 2-chlorobenzaldehyde (2.81 g, 20 mmol) in absolute ethanol (100 mL) was cooled to 0 °C and 2-acetylpyridine (2.42 g, 20 mmol) added. Aqueous sodium hydroxide (20 mL, 1.0 M) was then added dropwise and the reaction mixture stirred at 0 °C for 3 h. This resulted in the separation of a light yellow precipitate that was collected by filtration, washed with ethanol and dried *in vacuo*. Yield: 4.79 g, 98%. Anal. Calc. for $C_{14}H_{10}ClNO$: C 69.0; H 4.1; N 5.8. Found: C 68.9; H 4.1; N 5.8%. MS(EI) *m*/*z*: 244, M^+. IR (KBr, cm^{-1}): *ν*(CO) 1675s.

4′-(*o*-Chlorophenyl)-2,2′:6′,2″-terpyridine. *N*-{1-(2′-pyridyl)-1-oxo-2-ethyl}pyridinium iodide (0.68 g, 2.2 mmol) and ammonium acetate (10 g, excess) were added to a suspension of 2-chloro-1-{3-(2-pyridyl)-3-oxopropenyl}benzene (0.49 g, 2.0 mmol) in absolute ethanol (8 mL) and the mixture heated at reflux for 1.5 h. An off-white solid precipitated on cooling. This was collected by filtration, washed with 50% aqueous ethanol and dried *in vacuo*. Recrystallisation from ethanol afforded colourless crystals of the ligand. Yield: 0.38 g, 55%. Mp: 158–163 °C. Anal. Calc. for $C_{21}H_{14}ClN_3$: C 73.4; H 4.1; N 12.2. Found: C 73.4; H 4.2; N 12.2%. MS(EI) *m*/*z*: 343, M^+. ^{1}H NMR ($CDCl_3$): *δ* 8.71 (m, 2 H, $H_{6,6''}$); 8.68 (m, 2 H, $H_{3,3''}$); 8.57 (s, 2 H, $H_{3',5'}$); 7.84 (m, 2 H, $H_{4',4''}$); 7.51 (m, 4 H, C_6H_4); 7.35 (m, 2 H,

$H_{5,5''}$). UV-vis (20 μM in CH_3CN): λ_{max}/nm (ε/M^{-1} cm^{-1}): 303 (sh, 1.6×10^4); 277 (3.0×10^4); 246 (3.5×10^4).

[Pt{4′-(*o*-ClC_6H_4)trpy}Cl]SbF_6. A suspension of [$Pt(PhCN)_2Cl_2$] (0.10 g, 0.21 mmol) in acetonitrile (10 mL) was treated with an equimolar amount of $AgSbF_6$ (0.073 g) dissolved in acetonitrile (5 mL). The reaction mixture was heated under reflux for 16 h, the AgCl precipitate removed by filtration and one equivalent of 4′-(*o*-chlorophenyl)-2,2′:6′,2″-terpyridine (0.051 g) added to the filtrate. The reaction mixture was heated under reflux for an additional 24 h after which the volume was reduced *in vacuo*, the solution cooled to room temperature and allowed to stand for a further 24 h. This resulted in the precipitation of [Pt{4′-(*o*-ClC_6H_4)trpy}Cl]SbF_6. The precipitate was washed with cold acetonitrile (*ca.* 5 mL) and diethyl ether (*ca.* 10 mL) and dried *in vacuo* to afford an analytically pure microcrystalline product. Yield and colour: 0.16 g, 91%, orange. Anal. Calc. for $C_{21}H_{14}Cl_2F_6N_3PtSb$: C 31.1; H 1.9; N 5.2. Found: C 31.0; H 1.6; N 5.3%. IR (KBr, cm^{-1}): ν[4′-(*o*-ClC_6H_4)trpy]: 1610s, 1479m, 1418m, 1033m; $\nu(SbF_6^-)$ 658vs. ^{1}H NMR (DMSO-d_6): δ 8.89 (2H, d, $^3J_{HH}$ 5.5 Hz, $H_{6,6''}$) 8.86 (2H, s, $H_{3',5'}$) 8.71 (2H, d,$^3J_{HH}$ 8.2 Hz, $H_{3,3''}$) 8.50 (2H, t,$^3J_{HH}$ 7.8 Hz $H_{4,4''}$) 7.94 (2H, t,$^3J_{HH}$ 6.6 Hz $H_{5,5''}$) 7.65–7.81 (4H, m, phenyl CH). ^{13}C NMR (DMSO-d_6): δ 158.2 (2C, s, terpy quat. C) 154.2 (2C, s, terpy quat. C) 151.9 (1C, s, quat. C) 151.3 (2C, s, $C_{6,6''}$) 142.7 (2C, s, $C_{4,4''}$) 135.8 (1C, s, quat. C) 131.8 (1C, s, phenyl CH) 131.3 (1C, s, phenyl CH) 130.9 (1C, s, quat C) 130.3 (1C, s, phenyl CH) 129.3 (2C, s, $C_{5,5''}$) 128.1 (1C, s, phenyl CH) 126.0 (2C, s, $C_{4,4''}$) 125.2 (2C, s, $C_{3',5'}$). UV–vis (20 μM in CH_3CN): λ_{max}/nm (ε/M^{-1} cm^{-1}) 284 (3.5×10^4); 307 (1.7×10^4); 316 (1.6×10^4); 333 (1.8×10^4); 351 (8.0×10^3); 383 (4.1×10^3); 399 (4.4×10^3)].

Crystal structure determinations

Orange needle-shaped crystals of [Pt{4′-(*o*-ClC_6H_4)trpy}Cl]SbF_6 were grown by slow evaporation at room temperature of a saturated solution of the compound in acetonitrile. Crystal data and details of the crystallographic study are reported in Table 1. Intensity data were obtained on an Enraf-Nonius CAD4 diffractometer, using graphite monochromated Mo-Kα radiation and the ω–2θ scan technique. Unit cell parameters were obtained by least squares fitting of 25 reflections monitored in the range $3 < \theta < 12°$ while the diffraction data were collected in the range $2 < \theta < 23°$. For the low-temperature measurements the crystal was cooled in a stream of nitrogen supplied by a Bruker LT3 cryostat. Corrections for Lorentz, polarisation, and absorption (χ scans of 9 reflections) effects were applied. The intensities of three standard reflections showed no variations greater than those predicted by counting statistics. The structures were solved by Patterson and Fourier methods and refined by full-matrix least-squares using SHELXS-97[26] with all non-hydrogen atoms assigned anisotropic temperature factors and with the hydrogen atoms (in calculated positions) assigned a single overall isotropic temperature factor. The temperature factor for Cl(2) is exceptionally high (U_{eq} = 0.308 Å^2) with a difference Fourier indicating that this chlorine is disordered between two positions, one on each side of the plane of the phenyl ring. However, the disordered model was not used in the refinement as it brought no significant improvement to the *R*-factors nor did it add in any way to the interpretation of the stacking of the cations. The crystal structure diagrams were produced by the ORTEP program.[27]

CCDC reference numbers 194846–194849.

See http://www.rsc.org/suppdata/dt/b2/b209754k/ for crystallographic data in CIF or other electronic format.

Acknowledgements

We acknowledge financial support from the University of Natal and the South African National Research Foundation. Thanks also go to the United States National Research Foundation for funding through grant CHE 97-26435.

References

1 V. H. Houlding and V. M. Miskowski, *Coord. Chem. Rev.*, 1991, **111**, 145.
2 V. M. Miskowski and V. H. Houlding, *Inorg. Chem.*, 1989, **28**, 1529.
3 M. Weiser-Wallfahrer and G. Z. Gliemann, *Z. Naturforsch., Teil B*, 1990, **45**, 652.
4 V. M. Miskowski and V. H. Houlding, *Inorg. Chem.*, 1991, **30**, 4446.
5 V. M. Miskowski, V. H. Houlding, C-M. Che and Y. Wang, *Inorg. Chem.*, 1993, **32**, 2518.
6 H-K. Yip, L-K. Cheng, K-K. Cheung and C-M. Che, *J. Chem. Soc., Dalton Trans.*, 1993, 2933.
7 J. A. Bailey, M. G. Hill, R. E. Marsh, V. M. Miskowski, W. P. Schaefer and H. B. Gray, *Inorg. Chem.*, 1995, **34**, 4591.
8 W. B. Connick, L. M. Henling, R. E. Marsh and H. B. Gray, *Inorg. Chem.*, 1996, **35**, 6261.
9 R. Büchner, J. S. Field, R. J. Haines, C. T. Cunningham and D. R. McMillin, *Inorg. Chem.*, 1997, **36**, 3952.
10 R. Büchner, C. T. Cunningham, J. S. Field, R. J. Haines, D. R. McMillin and G. C. Summerton, *J. Chem. Soc., Dalton Trans.*, 1999, 711.
11 C-M. Che, L-Y. He, C-K. Poon and T. C. W. Mak, *Inorg. Chem.*, 1989, **28**, 3081.
12 W. B. Connick, L. M. Henling and R. E. Marsh, *Acta Crystallogr., Sect. B*, 1996, **52**, 1638.
13 M. Kato, C. Kosuge, K. Morii, J. S. Ahn, H. Kitagawa, T. Mitani, M. Matsushita, T. Kato, S. Yano and M. Kimura, *Inorg. Chem.*, 1999, **38**, 1638.
14 G. Gliemann and Y. Yersin, *Struct. Bonding (Berlin)*, 1985, **62**, 87.
15 J. S. Field, R. J. Haines, D. R. McMillin and G. C. Summerton, *J. Chem. Soc., Dalton Trans.*, 2002, 1369.
16 V. W. W. Yam, K. M. C. Wong and N. Zhu, *J. Am. Chem. Soc.*, 2002, **124**, 6506.
17 S. M. Drew, D. E. Janzen, C. E. Buss, D. I. MacEwan, K. M. Dublin and K. R. Mann, *J. Am. Chem. Soc.*, 2001, **123**, 8414; C. E. Buss and K. R. Mann, *J. Am. Chem. Soc.*, 2002, **124**, 1031; M. Kato, A. Omura, A. Toshikawa, S. Kishi and Y. Sugimoto, *Angew. Chem., Int. Ed.*, 2002, **17**, 3183.
18 F. Kröhnke, *Synthesis*, 1976, 1.
19 K. W. Jennette, J. T. Gill, J. A. Sadownick and S. J. Lippard, *J. Am. Chem. Soc.*, 1976, **98**, 6159; J. A. Bailey, V. M. Miskowski and H. B. Gray, *Acta Crystallogr., Sect. C.*, 1992, **48**, 1420.
20 D. S. Martin, in *Extended Interactions between Metal Ions*, ed. L. V. Interannte, *ACS Symp. Ser. 5*, American Chemical Society, Washington, DC, 1974, p. 254.
21 D. K. Crites and D. R. McMillin, *Coord. Chem. Rev.*, 2001, **211**, 195.
22 W. B. Connick, R. E. Marsh, W. P. Schaefer and H. B. Gray, *Inorg. Chem.*, 1997, **36**, 913.
23 R. E. Peierls, *Quantum Theory of Solids*, Oxford, London, 1953.
24 L. Carlsen, H. Egsgaard and J. R. Anderson, *Anal. Chem.*, 1979, **51**, 1593.
25 F. Liu, K. L. Cunningham, W. Uphues, G. W. Fink, J. Schmolt and D. R. McMillin, *Inorg. Chem.*, 1995, **34**, 2015; K. L. Cunningham, C. R. Hecker and D. R. McMillin, *Inorg. Chim. Acta.*, 1996, **242**, 143.
26 G. M. Sheldrick, SHELXS-97, A program for crystal structure determination and refinement, University of Göttingen, 1997.
27 L. Farrugia, *J. Appl. Crystallogr.*, 1997, **30**, 565.